Fractal scaling and crack-size effects on creep crack growth

Alberto CARPINTERI[1], Gianni NICCOLINI[1], Alessio RUBINO[1]

[1]Department of Structural, Geotechnical and Building Engineering,

Politecnico di Torino, Corso Duca degli Abruzzi 24, 10129 Torino, Italy

Email: alberto.carpinteri@polito.it, gianni.niccolini@polito.it,

alessio.rubino@polito.it (Corresponding author)

Abstract

Scaling effects on the creep crack growth behaviour are investigated by analyzing the results of compact tension (CT) tests on different-sized notched steel specimens appearing in the literature. Creep crack growth rate data are correlated to the elastic stress-intensity factor in terms of a Paris-type law, $\mathrm{d}a/\mathrm{d}t = C_0\, K^q$, where C_0 turns out to be a crack-size dependent coefficient of proportionality. Considering specimens with the same loading configuration (CT) and the same thickness, the observed crack-size effect on the creep crack growth rate is discussed on the basis of self-similarity considerations, and geometrically interpreted in terms of fractal tortuosity of the crack profile. A size-independent formulation of the creep crack growth law correlating renormalized quantities is finally deduced and confirmed by the experimental results.

Keywords: creep crack growth; scaling effects; incomplete self-similarity; fractal geometry; renormalization group theory.

1 Introduction

Design and integrity assessment of structural components operating at high temperatures have typically to account for the creep behaviour under steady-state conditions, where the strain rate $\dot{\varepsilon}$ strongly depends on the applied stress σ according to the Norton law [1,2]:

$$\dot{\varepsilon} = A\,\sigma^n, \tag{1}$$

where A and n, the latter being known as creep sensitivity [3], are temperature-dependent material parameters.

Actually, failure of structural components operating under creep conditions can occur by either creep rupture or creep crack growth. The former is most likely in components which are initially flaw-free or containing benign defects. However, the presence of inherent sharp defects, which can grow and ultimately cause brittle fracture, has necessitated characterizing the creep crack growth as well, often relegating the "flaw-free" condition to a mere idealization.

Despite the predictive character of fracture mechanics, whereby the results from laboratory specimens can be extrapolated to make predictions on full-sized structural components, and the number of studies conducted about creep, only a few of them were directly aimed at investigating size effects. In the current paper, the approach of fracture mechanics is supplemented by self-similarity and fractal geometry considerations to re-examine the observed crack-size effects on the creep crack growth behaviour for metallic materials.

2 Characterizations of creep crack growth by Fracture Mechanics

To properly identify a fracture parameter able to account for creep in the crack growth behaviour, a schematic representation of the creep deformation process in a cracked body has been considered. Immediately after loading, $r^{-1/2}$-type (being r the distance from the crack tip) and HRR [4,5] singular stress distributions are respectively generated in linear elastic and power-law hardening materials. In either case, if extensive creep deformation has had time to increase in size before the crack propagation, neither the elastic stress-intensity factor, K, nor the J-integral [6,7] —characterizing the HRR solution— can adequately characterize the crack-tip stress field. That is due to the nonlinear and time-dependent character of creep deformation, which is not admitted in linear elastic fracture mechanics (LEFM) and elastic-plastic fracture mechanics (EPFM) formulations [8-10].

By analogy with the J-integral, Landes and Begley [11], Nikbin et al. [12] defined the C^*-integral as a path-independent crack-tip parameter characterizing stress and strain rate fields when creep strains dominate:

$$C^* = \int_\Gamma \; W^* \, \mathrm{d}y - t_i(\partial \dot{u}_i/\partial x)\mathrm{d}s, \qquad (2)$$

(being $W^* = \int_0^{\dot{\varepsilon}_{ij}} \sigma_{ij}\, \mathrm{d}\, \dot{\varepsilon}_{ij}$ the strain energy density rate, Γ a contour surrounding the crack tip, $\boldsymbol{t}$ the traction vector, and $\dot{\boldsymbol{u}}$ the displacement rate vector)

$$\sigma_{ij} \propto (C^*/r)^{1/(n+1)}, \tag{3.a}$$

$$\dot{\varepsilon}_{ij} \propto (C^*/r)^{n/(n+1)}. \tag{3.b}$$

By comparing with the HRR solution, the analogy between creeping and power-law hardening materials is apparent.

Several studies [11,13-16] demonstrated that the creep crack growth rate (CCGR) can be described by an expression of the form:

$$\frac{\mathrm{d}a}{\mathrm{d}t} = D_0\, C^{*\,\phi}, \tag{4}$$

where D_0 is a material constant and $\phi \lesssim 1$. It can be noted that for intermediate values of the creep sensitivity n, CCGR data are correlated to the C^*-integral according to Eq.(4) [8,10].

More recently, extensive work in the field of time-dependent fracture mechanics (TDFM) has been devoted to the analysis of the so-called constraint effects on CCGR. In analogy with EPFM [17-19], results of recent research have extended TDFM beyond the limits of single-parameter theory, where a two-parameter (C*-

Q) approach has been proposed to characterize crack-tip constraint at elevated temperatures [19-22]. The Q parameter is introduced for quantifying the constraint effects during creep, in terms of deviations of the actual crack-tip stress-field —generally determined by numerical FEM analysis— from the HRR field in Eq. (3). Numerical and experimental studies reported in the literature [23-32] regard the dependence of these effects on loading configuration [27,28,31], as well as crack depth [23,26,29] (in-plane constraint effects), and specimen thickness (out-of-plane constraint effects) [24-25]. The general conclusion is that higher constraint levels at the crack tip provide higher creep cracking rates.

Within the single-parameter assumption, several parameters have been hystorically proposed for characterizing the creep crack growth behaviour, as reported for instance in [12,33]. It was emphasized that for creep-ductile materials, defined as those in which the creep crack growth rate is negligible compared to the creep zone expansion rate, the creep zone completely engulfs the uncracked ligament before the crack actually propagates, causing extensive stress redistribution [8-10]. This circumstance occurs in highly susceptible materials to creep deformation, i.e. when $n \gg 1$ [3], whereby the crack-tip singularity tends to disappear according to Eq.(3.a). That makes a description in terms of net section stress or reference stress σ_{N} appropriate [34,35]:

$$\frac{\mathrm{d}a}{\mathrm{d}t} = B_0\, \sigma_{\mathrm{N}}{}^{s}, \tag{5}$$

where B_0 and s are material parameters.

A relevant attempt [36-39] to consider creep as a thermally activated process led to the following Arrhenius-type relationship:

$$\frac{\mathrm{d}a}{\mathrm{d}t} \propto \exp Q^*, \tag{6}$$

where Q^* is a function dependent upon the applied stress, the absolute temperature T, the specimen size b, the gas constant R, and the activation energy ΔH_f for crack extension. As regards the size-scale effects, the Authors found a power-law dependence of the CCGR on the specimen size b.

When a little creep deformation accompanies crack growth, the initial stress distribution remains virtually unaltered by creep, and K (or J) continues to characterize the stress state around the crack tip. Such creep-brittle behaviour, defined as that in which the creep crack growth rate da/dt is comparable to the creep zone expansion rate [8-10], occurs in case of high CCGR values when the specimen always remains in small-scale creep condition. For this circumstance, occurring at short times (when the stress-strain response is predominantly elastic) or for materials designed to resist large-scale creep deformations (i.e. with creep sensitivity $n \cong 1$), the creep crack growth rate is satisfactorily described in terms of stress-intensity factor K by means of a Paris-type law [40,41]:

$$\frac{\mathrm{d}a}{\mathrm{d}t} = C_0\, K^q, \tag{7}$$

where C_0 and q are material parameters.

Hereinafter, the attention will be focused on a set of CCGR data from an experimental campaign on CT steel specimens, originally correlated to both C^* and K [47]. Despite CCGR is currently interpreted in terms of C^* in the framework of constraint effects for most practical situations, on that occasion some success was found in correlating CCGR data to the elastic stress-intensity factor, K. In this case, the observed shift of the experimental curves is compatible with a crack-size effect, which can be interpreted in terms of self-similarity and fractal tortuosity of the crack profile, along the line of recent studies on fatigue crack growth [42-46].

3 Experimental characterization of creep crack growth

The creep crack growth behaviour of CT 1% CrMoV steel specimens of various sizes —standard and ultra-large specimens respectively of 50.8 mm and 254 mm in width, with thickness ranging from 6.35 to 63.5 mm— was investigated by Tabuchi et al.[47]. After introducing a fatigue pre-crack of 3 mm for standard specimens and of 15 mm for ultra-large specimens at room temperature, the Authors conducted creep crack growth tests at 538 °C. The tested geometry is outlined in Fig. 1, where the markers indicate the specimens under investigation. In this paper, the analysis is restricted to specimens with the same thickness (12.7 mm), and differing in width, i.e. in the initial crack length (3 and 15 mm), in order to isolate the crack-size effects on the CCGR.

The Authors discussed the experimental data both in the framework of TDFM and of LEFM, correlating satisfactorily creep crack growth rate by Eqs.(4) and (7), respectively. Characterization of da/dt in terms of the C^*-integral pointed out increasing creep crack growth rate with increasing specimen thickness, whereas neither specimen-width nor crack-size effects were observed. The specimen-thickness effect was already interpreted in the framework of the constraint effects, whereby the achievement of plane-strain conditions in very thick sections result in less creep ductility and higher cracking rates. Instead, lack of crack-size (or specimen-width) effects on creep crack growth rate was considered surprising, given that pre-crack of ultra-large specimens was five times longer than standard ones, and worthy of further investigation.

Actually, the characterization of creep crack growth rate in terms of K by Eq.(7) did not demonstrated thickness effects for specimens with the same width, but, rather, a right- and downward shift of CCGR data with increasing specimen width, or pre-crack length. The power-law exponent q of the two fitting curves varies over the range 14.1-14.7 (the average exponent is $\bar{q}$ = 14.4 ± 0.4. As shown in Fig. 2, da/dt for ultra-large specimens was about 1000 times lower than that for standard specimens for a given value of K. That may be interpreted as a crack-size effect whereby creep crack growth rate increases by decreasing the crack size, similarly to what happens with Paris law [42-46]. As a straightforward consequence, short cracks under creep conditions are expected to propagate at higher rates.

4 Generalized creep crack growth law

From a physical point of view, correlating creep crack growth rate d*a*/d*t* by an expression in the form of Eqs.(4), (5) or (7) provides little information on the multiple factors that affect creep crack growth. In the case of the above results, where CCGR data are satisfactorily correlated to K, a functional dependence upon a series of LEFM parameters can be properly stated:

$$\frac{\mathrm{d}a}{\mathrm{d}t} = \Phi(\sigma, K, T;\ \sigma_\mathrm{u}, K_\mathrm{C}, K_\mathrm{th}, X, T_\mathrm{M}; a), \tag{8}$$

In particular, the governing parameters include (i) a threshold value K_th of the stress-intensity factor, below which creep crack growth does not occur [48], (ii) the thermal diffusivity X $(\mathrm{m}^2\mathrm{s}^{-1})$ which controls the stress-induced migration of vacancies responsible for creep deformation, and (iii) the absolute melting temperature T_M of the material (creep is commonly found to become severe when the operating temperature exceeds $0.4\,T_\mathrm{M}$). It is worth noting that the loading configuration and the specimen thickness are not included as variable parameters, since geometry (CT) and thickness (Fig. 1) are fixed in the current analysis.

Considering $\sigma_{\mathrm{u}}, K_{\mathrm{C}}, X, T_{\mathrm{M}}$ as independent variables, the dimensional analysis [49] yields the following expression in terms of dimensionless parameters:

$$\frac{\mathrm{d}a}{\mathrm{d}t} = \frac{X}{a_0}\Phi_1\left(\frac{\sigma}{\sigma_{\mathrm{u}}}, \frac{K}{K_{\mathrm{C}}}, \frac{K_{\mathrm{th}}}{K_{\mathrm{C}}}, \frac{T}{T_{\mathrm{M}}}, \frac{a}{a_0}\right), \tag{9}$$

where a_0 represents the fracture sensitivity of the material as a function of the fracture toughness K_{C} and tensile strength σ_{u}, $a_0 = (K_{\mathrm{C}}/\sigma_{\mathrm{u}})^2/\pi$.

On the other hand, power-law relationships, such as those presented to describe creep crack growth rate, give the evidence of self-similarity, wherein a phenomenon reproduces itself over different time and space scales. It has been observed that self-similar solutions describe the intermediate asymptotic behaviour of fatigue crack growth when "the influence of the initial conditions has disappeared but the influence of the instability has not yet intruded" [50-53].

Accordingly, characterization of creep crack growth in terms of power laws is signature of an intermediate asymptotic regime, which is achieved in the mid-range of growth rates, i.e., when the crack has started to propagate although the material is sufficiently far from failure. The so-called incomplete self-similarity prevails at this stage, corresponding to a power-law dependence of creep crack growth rate on certain dimensionless parameters.

Let us consider a and K. Since the above experimental evidences have shown the dependence of the creep crack growth rate on a and K, incomplete self-similarity is assumed in the corresponding dimensionless parameters a/a_0 and K/K_C. Thus, Eq.(9) takes the following power-law asymptotic form:

$$\frac{\mathrm{d}a}{\mathrm{d}t} = \frac{X}{a_0}\Phi_2\left(\frac{\sigma}{\sigma_\mathrm{u}},\frac{K_\mathrm{th}}{K_\mathrm{C}},\frac{T}{T_\mathrm{M}}\right)\left(\frac{a}{a_0}\right)^{\gamma_2}\left(\frac{K}{K_C}\right)^{\gamma_1} \equiv C_0\, K^{\gamma_1}. \tag{10}$$

Comparing the generalized creep crack growth law of Eq.(9) with Eq.(7) gives:

$$\gamma_1 = q \tag{11.a}$$

$$C_0 \equiv \frac{X}{a_0}\Phi_2\left(\frac{\sigma}{\sigma_\mathrm{u}},\frac{K_\mathrm{th}}{K_\mathrm{C}},\frac{T}{T_\mathrm{M}}\right)\left(\frac{a}{a_0}\right)^{\gamma_2} {K_C}^{-\gamma_1} \tag{11.b}$$

Eq.(10) is formally identical to the classical Paris-type law in Eq.(7) for creep crack growth, but the coefficient of proportionality C_0 is not simply a function of the material properties and temperature, but turns out to depend on the actual crack length a as well. The exponent γ_2 governing such size effect cannot be obtained from the dimensional analysis, but rather using experimental data.

Deviations from the mid-range power-law behaviour, predictable within intermediate asymptotics, have been experimentally verified [48] when the conditions of non-propagating crack, for $K \to K_{\text{th}}$, and Griffith-Irwin instability, for $K \to K_{\text{C}}$, are approached, yielding a Paris-type curve illustrated in Fig. 3.

5 Fractal approach to creep crack growth

Since the publication of the celebrated article by Mandelbrot and co-workers [54], the fractal nature of metal fracture surfaces has been widely recognized. Such a fractal character has been revealed also for metallic substructures under creep conditions [55,56]. Repeated observations at various magnifications have shown that the structure replicates itself in a self-similar way in a range of intermediate scales, falling between the micro-scale —influenced by grains, inclusions and dislocations— and the macro-scale — characterized by the size of the specimen and the notch from which the crack propagates. Accordingly, a geometric interpretation of crack-size effects on the creep crack growth rate is obtained in the context of fractal geometry [57,58], whereby the crack profile can be modelled as an invasive fractal set a^*, with projected length a and topological dimension $1 + d_{\mathcal{G}}$ $(0 < d_{\mathcal{G}} < 1)$:

$$a^* \simeq a^{1+d_{\mathcal{G}}}. \tag{12}$$

On the other hand, revisiting the Griffith energy balance in the context of fractal cracks yields the following scaling law:

$$K \simeq K^* a^{d_{\mathcal{G}}/2}\,, \tag{13}$$

where K^* is the renormalized stress-intensity factor with anomalous physical dimensions $[F][L]^{-(3+d_{\mathcal{G}})/2}$.

Exploiting Eq.(12), an application of the derivation rule for composite functions gives:

$$\frac{\mathrm{d}a}{\mathrm{d}t} = \frac{\mathrm{d}a}{\mathrm{d}a^*}\frac{\mathrm{d}a^*}{\mathrm{d}t} = \frac{\mathrm{d}a^*}{\mathrm{d}t}\frac{a^{-d_{\mathcal{G}}}}{1+d_{\mathcal{G}}}. \tag{14}$$

Inserting Eqs. (13) and (14) into Eq.(7) yields:

$$\frac{\mathrm{d}a^*}{\mathrm{d}t}\frac{a^{-d_{\mathcal{G}}}}{1+d_{\mathcal{G}}} = C_0 K^{*q} a^{d_{\mathcal{G}}q/2}. \tag{15}$$

Analogously to fractal fatigue models [42-46], if the following scale-invariant relationship between fractal quantities is assumed for creep crack growth:

$$\frac{\mathrm{d}a^*}{\mathrm{d}t} = C_0^*\, K^{*q}, \tag{16}$$

Eq. (15) reduces to:

$$C_0(a) = \frac{C_0^*}{(1 + d_{\mathcal{G}})} a^{-d_{\mathcal{G}}(1+q/2)}, \tag{17}$$

which returns by another route the crack-size dependency of the coefficient C_0 as in Eqs.(10) and (11.b). Comparing Eqs.(11.b) and (17) gives $\gamma_2 = -d_{\mathcal{G}}(1 + q/2)$. Note that Eq.(17) predicts a negative scaling of C_0 due to fractal roughness of the crack profile (i.e., for $d_{\mathcal{G}} > 0$). Accordingly, the creep crack growth rate da/dt in Eq.(7) is a decreasing function of the crack length as pointed out by the aforementioned experimental results. It should be noted that by combining the two scaling behaviours of $\mathrm{d}a/\mathrm{d}t$ and K with respect to the crack size a —see Eqs.(13) and (14) — it is possible to predict the right- and downward shift of CCGR curves. The experimental CCGR curves (with da/dt in mm h^{-1} and K in MPa $\mathrm{m}^{1/2}$) are renormalized by a transformation of the axes K and $\mathrm{d}a/\mathrm{d}t$ of the form, $K \rightarrow K^* = K\, a^{-d_{\mathcal{G}}/2}$ and $\mathrm{d}a/\mathrm{d}t \rightarrow \mathrm{d}a^*/\mathrm{d}t = (1 + d_{\mathcal{G}})a^{d_{\mathcal{G}}}\, \mathrm{d}a/\mathrm{d}t$, where a is equal to 3 and 15 mm. The renormalized data collapse onto a single line (shown in Fig. 4), illustrating the fulfilment of the crack-size independent creep crack growth law given by Eq.(16). The dimensional increment $d_{\mathcal{G}}$ of the crack profile is adjusted to achieve the best data collapse, yielding $d_{\mathcal{G}} = 0.58 \pm 0.09$ and, contextually, the following scale-invariant law:

$$\frac{\mathrm{d}a^*}{\mathrm{d}t} = 10^{-25.8}\, K^{*14.4}. \tag{18}$$

6 Discussion and conclusions

Experimental data about creep crack propagation for specimens with a pre-existing sharp defect are re-examined, revealing a clear crack-size effect on cracking rates when correlated to the elastic stress-intensity factor, K. These findings are formalized in the framework of dimensional analysis and intermediate asymptotics, leading to a generalized formulation of the creep crack growth law, $\mathrm{d}a/\mathrm{d}t = C_0\, K^q$, where the effects of the initial crack length as well of multiple parameters are taken into account. An application of the fractal geometry leads to the definition of a scale-invariant law, $\mathrm{d}a^*/\mathrm{d}t = C_0^*\, K^{*q}$, able to uniquely characterize the creep crack growth behaviour of the material, regardless of the size scale. Similarly to fatigue crack propagation (where analogous scaling laws are obtained by the change of variable $t \rightarrow N$, i.e., time $\rightarrow$ number of cycles), fractal roughness of the crack surfaces —through the dimensional increment $d_{\mathcal{G}}$— is predicted to be responsible for the negative scaling of C_0, whereby short cracks propagate at higher rates according to the experimental evidence.

Assuming for K_{th} the same scaling effect as for K_{C} and K, $K_{\mathrm{th}} = K_{\mathrm{th}}^*\, a^{d_{\mathcal{G}}/2}$, the shift of the nominal CCGR curves with crack size, as represented in Fig. 5(a), is obtained. Then, the collapse of the renormalized curves onto a Paris-type scaling function (solely material and temperature dependent) of Fig. 5(b) is an obvious consequence.

Extensive experimental work has to be conducted to confirm the present fractal approach. In particular, the investigation of a threshold limit, below which creep crack growth does not occur (see dashed branch of Paris-type curves in Fig.5), is related to the ability to inspect smaller and smaller cracks. Further studies could also concern the application of fractal geometry concepts to interpret crack-size effects on creep crack growth rate in terms of the C^*-integral.

References

[1] Garofalo F. (1965) *Fundamentals of Creep and Creep-Rupture in Metals*. Macmillan Series in Materials Science.

[2] Webster G.A., Ainsworth R.A. (1994) *High Temperature Components Life Assessment*. London: Chapman and Hall.

[3] Smith D.J., Webster G.A. (1981) Characterizations of creep crack growth in 1 per cent Cr Mo V steel. *Journal of Strain Analysis,* 16(2), 137-143.

[4] Hutchinson J.W. (1968) Singular behaviour at the end of a tensile crack in a hardening material. *Journal of the Mechanics and Physics of Solids*, 16(1), 13-31.

[5] Rice J.R., Rosengren G.F. (1968) Plane strain deformation near a crack tip in a power-law hardening material. *Journal of the Mechanics and Physics of Solids*, 16(1), 1-12.

[6] Cherepanov G. P. (1967) The propagation of cracks in a continuous medium. *Journal of Applied Mathematics and Mechanics*, 31(3), 503-512.

[7] Rice J.R. (1968) A path independent integral and the approximate analysis of strain concentration by notches and cracks. *Journal of Applied Mechanics*, 35, 379-386.

[8] Grover P.S., Saxena A. (1995) Creep crack growth in power plant materials. *Sadhana*, 20(1), 53-85.

[9] Saxena, A. (2003) Analysis of cracks under creep conditions. In: *Comprehensive Structural Integrity* (Edited by I. Milne, R.O. Ritchie and B. Karihaloo) Vol. 5: *Creep and High-Temperature Failure* (Edited by A. Saxena). Elsevier Ltd., Oxford, United Kingdom, 201-240.

[10] Webster, G.A. (2003) Creep crack growth. In: *Comprehensive Structural Integrity* (Edited by I. Milne, R.O. Ritchie and B. Karihaloo) Vol. 5: *Creep and High-Temperature Failure* (Edited by A. Saxena). Elsevier Ltd., Oxford, United Kingdom, 241-271.

[11] Landes J.D., Begley J.A. (1976) A fracture mechanics approach to creep crack growth. *ASTM Special Technical Publication* 590, 128-148.

[12] Nikbin K.M., Webster G.A., Turner C.E. (1976) Relevance of nonlinear fracture mechanics to creep cracking. *ASTM Special Technical Publication* 601, 47-62.

[13] Harper M.P., Ellison E.G. (1977) The use of C* parameter in predicting creep crack propagation rates. *Journal of Strain Analysis*, 12(3), 167-179.

[14] Nikbin K.M., Webster G.A., Turner C.E. (1977) A comparison of methods of correlating creep crack growth. In: *Fracture*, Vol. 2 of the *Proceedings of the 4th International Conference on Fracture* (*ICF4*), 19-24 June 1977, Waterloo, Canada, 627-634.

[15] Saxena A. (1980) Evaluation of C* for the characterization of creep crack growth behaviour in 304 SS. *ASTM Special Technical Publication* 700, 131-151.

[16] Riedel H., Rice J.R. (1980) Tensile cracks in creeping solids. *ASTM Special Technical Publication* 700, 112-130.

[17] O'Dowd N.P., Shih C.F. (1991) Family of crack-tip fields characterized by a triaxiality parameter — I. Structure of fields. *Journal of the Mechanics and Physics of Solids*, 39(8), 989-1015.

[18] O'Dowd N.P., Shih C.F. (1992) Family of crack-tip fields characterized by a triaxiality parameter — II. Fracture applications. *Journal of the Mechanics and Physics of Solids*, 40(5), 939-963.

[19] Shih C., O'Dowd N., Kirk M. (1993) A framework for quantifying crack tip constraint. In: *Constraint Effects in Fracture* (Edited by E. Hacklett, K. Scwalbe, and R. Dodds). ASTM International, 1993, 2-20.

[20] Budden P., Ainsworth R. (1999) The effect of constraint on creep fracture assessment. *International Journal of Fracture*, 97(1-4), 237-247.

[21] Bettinson A.D., O'Dowd N.P., Nikbin K. (2001) Two parameter characterization of crack tip fields under creep conditions. In: *Proceedings of the IUTAM Symposium*, 3-7 April 2000, Nagoya, Japan, 95-104.

[22] Nikbin K. (2004) Justification for meso-scale modelling in quantifying constraint during creep crack growth. *Materials Science and Engineering: A*, 365(1-2), 107-113.

[23] Sun P.J., Wang G.Z., Xuan F.Z., Tu S.T., Wang Z.D. (2011) Quantitative characterization of creep constraint induced by crack depths in compact tension specimens. *Engineering Fracture Mechanics*, 78(4), 653-665.

[24] Sun P.J., Wang G.Z., Xuan F.Z., Tu S.T., Wang Z.D. (2012) Three-dimensional numerical analysis of out-of-plane creep crack-tip constraint in compact tension specimens. *International Journal of Pressure Vessels and Piping*, 96-97, 78-89.

[25] Tan J.P., Tu S.T., Wang G.Z., Xuan F.Z. (2013) Effect and mechanism of out-of-plane constraint on creep crack growth behavior of a Cr-Mo-V steel. *Engineering Fracture Mechanics*, 99, 324-334.

[26] Wang G.Z., Liu X.L., Xuan F.Z., Tu S.T. (2010) Effect of constraint induced by crack depth on creep crack-tip stress field in CT specimens. *International Journal of Solids and Structures*, 47(1), 51-57.

[27] Wang G.Z., Li B.K., Xuan F.Z., Tu S.T. (2012) Numerical investigation on the creep crack-tip constraint induced by loading configuration of specimens. *Engineering Fracture Mechanics*, 79, 353-362.

[28] Zhang J.W., Wang G.Z., Xuan F.Z., Tu S.T. (2014) Prediction of creep crack growth behavior in Cr-Mo-V steel specimens with different constraints for a wide range of C^*. *Engineering Fracture Mechanics*, 132, 70-84.

[29] Zhao L., Jing H., Xu L., Han Y., Xiu J. (2012) Evaluation of constraint effects on creep crack growth by experimental investigation and numerical simulation. *Engineering Fracture Mechanics*, 96, 251-266.

[30] Zhao L., Jing H., Xiu J., Han Y., Xu L. (2014) Experimental investigation of specimen size effect on creep crack growth behavior in P92 steel welded joint. *Materials and Design*, 57, 736-743.

[31] Zhao L., Xu L., Han Y., Jing H. (2015) Quantifying the constraint effect induced by specimen geometry on creep crack growth behavior in P92 steel. *International Journal of Mechanical Sciences*, 94-95, 63-74.

[32] Zhao L., Xu L., Han Y., Jing H. (2015) Two-parameter characterization of constraint effect induced by specimen size on creep crack growth. *Engineering Fracture Mechanics*, 143, 121-137.

[33] Van Leeuwen, H.P. (1977) The application of fracture mechanics to creep crack growth. *Engineering Fracture Mechanics*, 9, 951-974.

[34] Harrison C.B., Sandor G.N. (1971) High-Temperature crack growth in low-cycle fatigue. *Engineering Fracture Mechanics*, 3, 403-420.

[35] Nicholson R.D., Formby C.L. (1975) The validity of various fracture mechanics methods at creep temperatures. *International Journal of Fracture*, 11(4), 595-604.

[36] Yokobori A.T., Yokobori T., Kuriyama T., Kako T., Kaji Y. (1986) Characterization of high temperature creep crack growth rate in terms of independent parameters. In: *Proceedings of the International Conference on Creep*, 14-18 April 1986, Tokyo, Japan, 135-140.

[37] Yokobori A.T., Yokobori T. (1989) New concept to crack growth at high temperature creep and creep-fatigue. In: *Advances in Fracture Research*, Vol. 2 of

the *Proceedings of the 7th International Conference on Fracture* (*ICF7*), 20-24 March 1989, Houston, Texas, 1723-1735.

[38] Yokobori A.T., Yokobori T., Nishihata T., Yamaoka T. (1992) An alternative correlating parameter for creep crack growth rate and its application: Derivation of the parameter Q^*. *Materials at High Temperatures*, 10, 108-118.

[39] Yokobori A.T., Yokobori T. (1996) Comparative study on characterization parameters for high temperature creep crack growth with special emphasis on dual value behaviour of crack growth rate. *Engineering Fracture Mechanics*, 55, 493-503.

[40] Siverns M.J., Price A.T. (1970) Crack growth under creep conditions. *Nature*, 228, 760-761.

[41] Siverns M.J., Price A.T. (1973) Crack propagation under creep conditions in a quenched 2.25 chromium 1 molybdenum steel. *International Journal of Fracture*, 9(2), 199-207.

[42] Carpinteri An., Spagnoli A. (2004) A fractal analysis of size effect on fatigue crack growth. *International Journal of Fatigue*, 26, 125-133.

[43] Carpinteri A., Paggi M. (2010) A unified fractal approach for the interpretation of the anomalous scaling laws in fatigue and comparison with existing models. *International Journal of Fracture*, 161, 41-52.

[44] Carpinteri A., Montagnoli F. (2019) Scaling and fractality in fatigue crack growth: Implications to Paris' law and Wöhler's curve. *Procedia Structural Integrity*, 14, 957-963.

[45] Carpinteri A., Montagnoli F. (2020) Scaling and fractality in sub-cirtical fatigue crack growth: Crack-size effects on Paris' law and fatigue threshold. *Fatigue & Fracture of Engineering Materials & Structures*, 43, 788-801.

[46] Paggi M., Carpinteri A. (2009) Fractal and multifractal approaches for the analysis of crack-size dependent scaling laws in fatigue. *Chaos, Solitons & Fractals*, 40, 1136-1145.

[47] Tabuchi M., Kubo K., Yagi K. (1991) Effect of specimen size on creep crack growth rate using ultra-large CT specimens for 1 Cr-Mo-V steel. *Engineering Fracture Mechanics*, 40, 311-321.

[48] Yokobori T., Sakata H. (1980) Studies on crack growth rate under high temperature creep, fatigue, and creep-fatigue interaction — I: On the experimental studies on crack growth rate as affected by $\alpha\sigma_{\mathrm{g}}$, σ_{g} and temperature. *Engineering Fracture Mechanics*, 13(3), 509-522.

[49] Buckingham E. (1915) Model experiments and the forms of empirical equations. *ASME Transactions*, 37, 263-296.

[50] Barenblatt G.I., Botvina L.R. (1980) Incomplete self-similarity of fatigue in the linear range of fatigue crack growth. *Fatigue and Fracture of Engineering Materials and Structures*, 3, 193-202.

[51] Barenblatt G.I. (1996) *Scaling, Self-similarity and Intermediate Asymptotics*. Cambridge: Cambridge University Press.

[52] Barenblatt G.I. (2006) Scaling phenomena in fatigue and fracture. *International Journal of Fracture*, 138, 19-35.

[53] Ritchie R.O. (2005) Incomplete self-similarity and fatigue-crack growth. *International Journal of Fracture*, 132, 197-203.

[54] Mandelbrot B.B., Passoja D.E., Paullay A.J. (1984) Fractal character of fracture surfaces of metals. *Nature*, 308, 721-722.

[55] Zaiser M., Bay K., Hähner P. (1999) Fractal analysis of deformation-induced dislocation patterns. *Acta Mater.*, 47, 2463-2476

[56] Fernández R., Bruno G., González-Doncel G. (2018) Fractal nature of aluminum alloys substructures under creep and its implications. *Journal of Applied Physics*, 123, 145108-1-145108-8.

[57] Carpinteri A. (1994) Fractal nature of material microstructure and size effects on apparent mechanical properties. *Mechanics of Materials*, 18, 89-101. Internal Report, Laboratory of Fracture Mechanics, Politecnico di Torino, N. 1/92, 1992.

[58] Carpinteri A. (1994) Scaling laws and renormalization groups for strength and toughness of disordered materials. *International Journal of Solids and Structures*, 31, 291-302.

Figure captions

Fig. 1. Geometry and size of CT specimens tested (adapted from [47])

Fig. 2. Shift of experimental CCGR curves correlating da/dt with K (adapted from [47]) for different initial crack lengths, accounting for the crack-size effect.

Fig. 3. Schematization of CCGR diagram: power-law stage corresponds to the intermediate asymptotic behaviour.

Fig. 4. Collapse of the renormalized CCGR data onto the fitting line represented by Eq.(18) in the fractal K^* *vs* $\mathrm{d}a^*/\mathrm{d}t$ diagram.

Fig. 5. Predicted nominal CCGR curves (*a*) and renormalized curve in the fractal diagram (*b*), where v_{th} (or $v_{\mathrm{th}}{}^*$) and v_{cr} (or $v_{\mathrm{cr}}{}^*$) denote threshold and critical CCGRs given by Eq.(14). The dashed line represents the region to be carefully investigated.

Figures

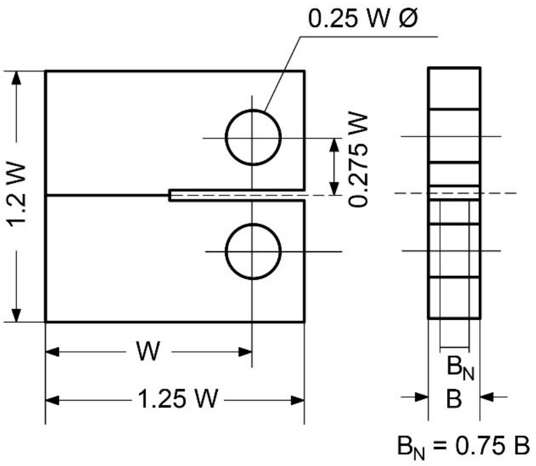

Test specimen

	W (mm)	B (mm)
	50.8	25.4
□	50.8	12.7
	50.8	6.35
	254.0	63.5
◆	254.0	12.7

Specimen size

Fig. 1.

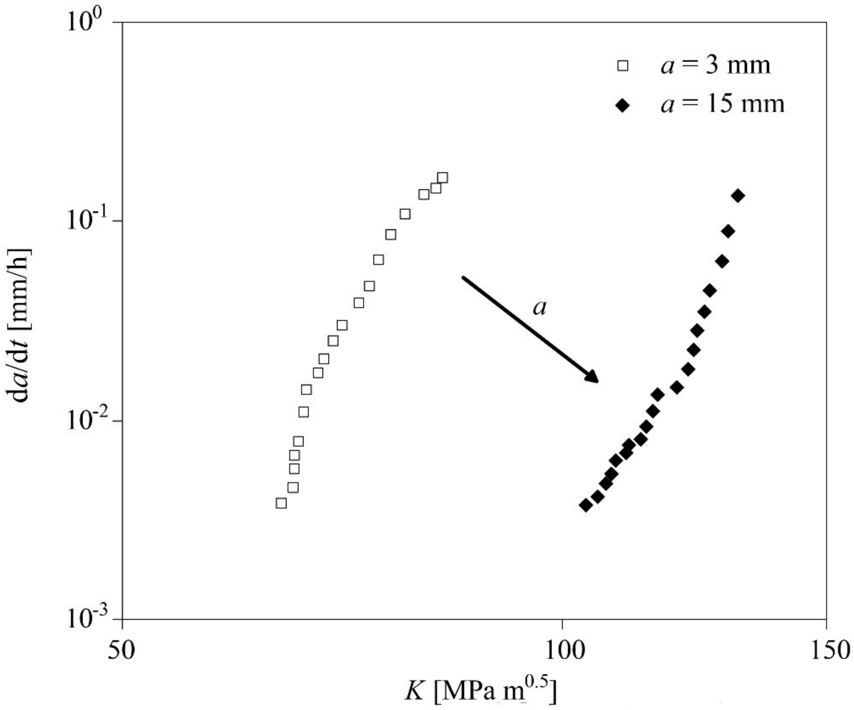

Fig. 2.

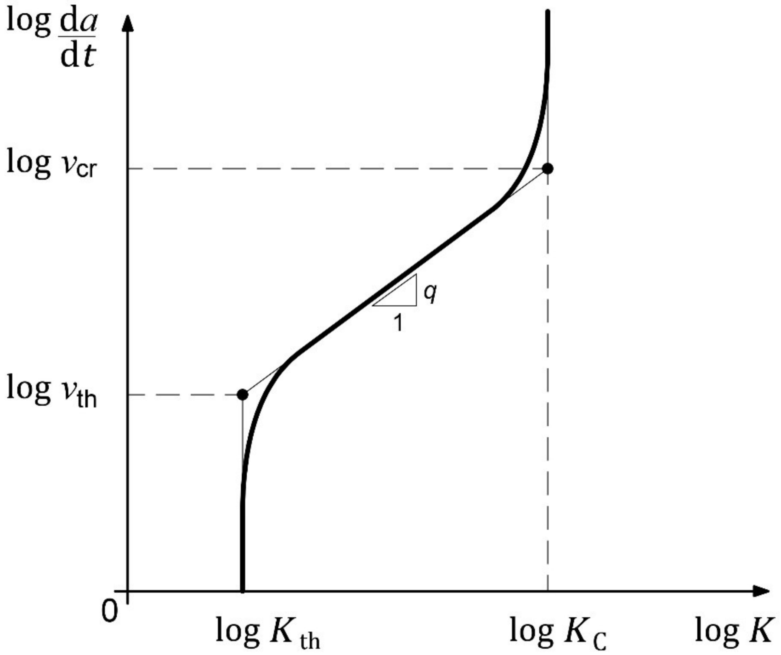

Fig. 3.

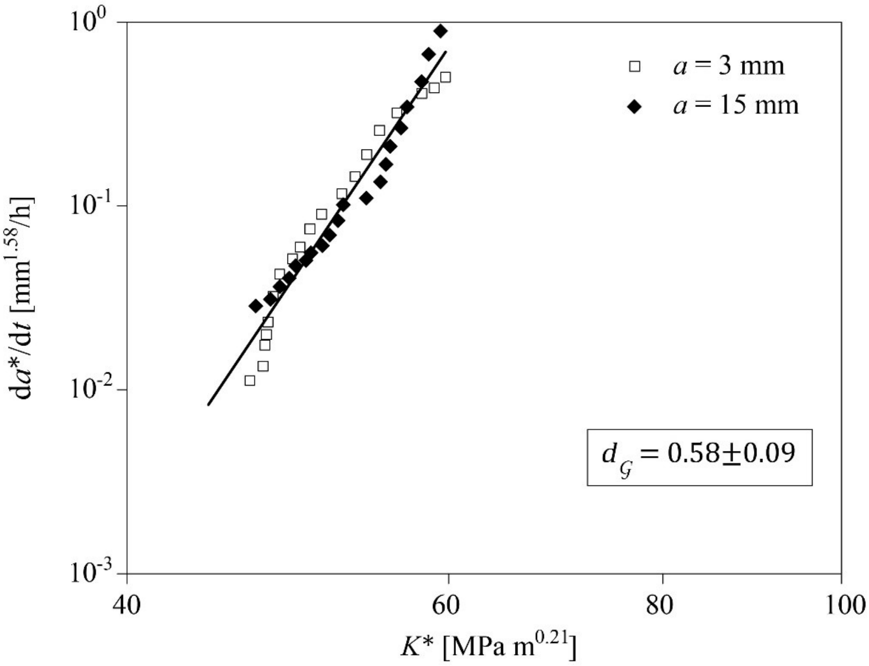

10^0
10^{-1}
10^{-2}
10^{-3}
da*/dt [mm$^{1.58}$/h]
40
60
80
100
K* [MPa m$^{0.21}$]
a = 3 mm
a = 15 mm
$d_{\mathcal{G}} = 0.58 \pm 0.09$

Fig. 4.

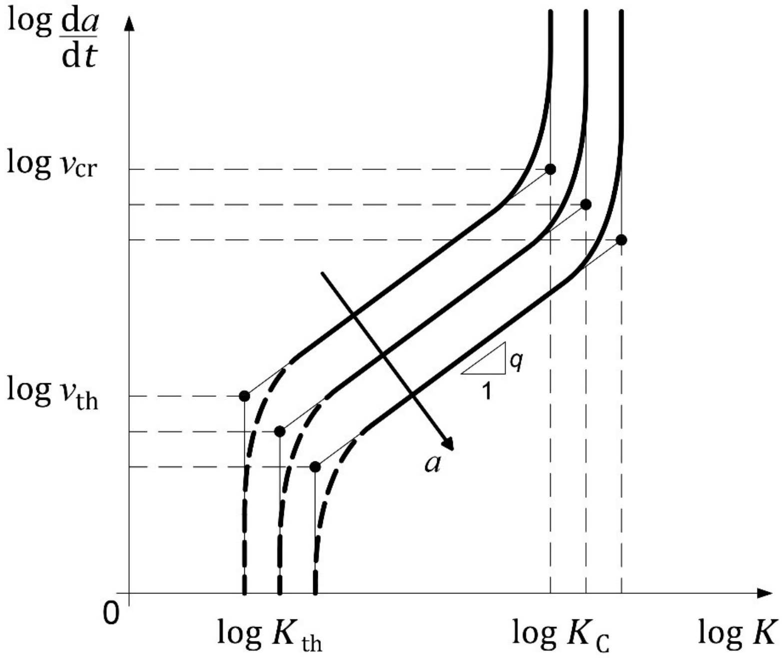

log $\frac{da}{dt}$
log v_{cr}
log v_{th}
q
1
a
0
log K_{th}
log K_C
log K

Fig. 5 (*a*)

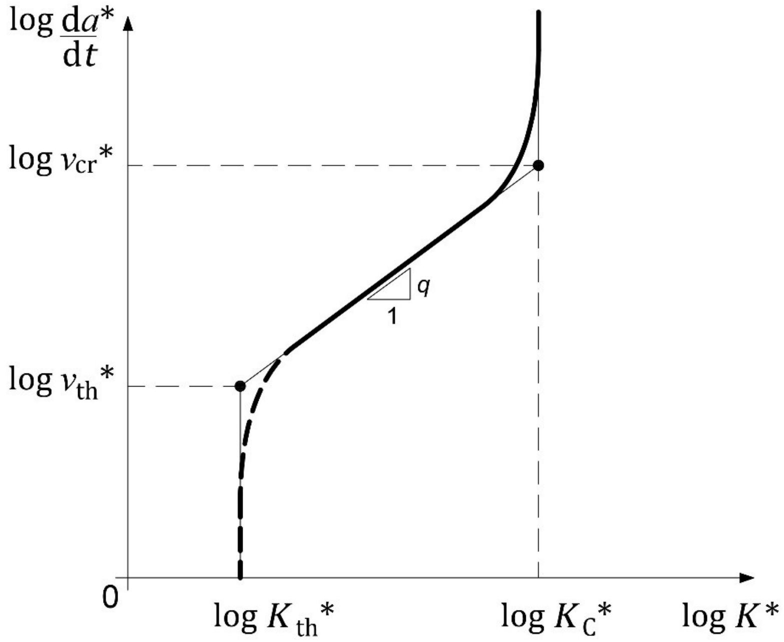

log $\frac{da^*}{dt}$
log v_{cr}*
log v_{th}*
q
1
0
log K_{th}*
log K_C*
log K*

Fig. 5 (*b*)